Optimization of Aluminum/Silicon Compounds on Fire Resistance of Old Corrugated Container Fiber Foam Material

Lili Cai,[a] Tingjie Chen,[a,b] Wei Wang,[a] Daobang Huang,[a] Qihua Wei,[a] Ming Lin,[a] and Yongqun Xie [a,*]

Old corrugated container fiber foam material (OCCM) was prepared using a liquid frothing approach. The effect of the content of Al/Si compounds, the molar ratio of Al^{3+}/SiO_2, and different addition form on the limited oxygen index (LOI) and residue percentage of OCCM was optimized using an orthogonal design. The fire resistance of OCCM was best when the content of Al/Si compounds was 900 mL, the molar ratio of Al^{3+}/SiO_2 was 1:1, and the aluminum sulfate solution was added first, followed by the separately added sodium silicate solution. Under these conditions, the LOI and residue percentage of OCCM reached 32.3 and 53.51%, respectively. Thermogravimetric analysis indicated that Al/Si compounds promoted char formation and reduced the heat release of the optimized OCCMs during depolymerisation. Compared with the control group, the residue percentage of optimized OCCM was increased from 12.49% to 37.98%. Fourier transform infrared spectroscopy identified the functional groups of Al/Si compounds in the optimized OCCMs, confirming that pyrolysis of the optimized OCCMs was affected by Al/Si compounds.

Keywords: Aluminum sulfate; Sodium silicate; Fire resistance; Fiber foam material; Orthogonal design

Contact information: a: Department of Material Science and Engineering, Fujian Agriculture and Forestry University, 350002, Fuzhou, Fujian, China; b: Division of Wood Technology and Engineering, Luleå University of Technology, SE-93187, Forskargatan 1, Skellefteå, Sweden;
** Corresponding author: fjxieyq@hotmail.com*

INTRODUCTION

The reuse of old corrugated containers (OCC) is a good strategy for substituting petroleum products and preserving forest resources. Many studies have been published regarding the use and properties of OCC fibers (Chen *et al.* 2012; Heydari *et al.* 2013; Rahmaninia and Khosravani 2015; Tang *et al.* 2015), confirming the presence of a large interest in this field. However, the use of OCC fibers as a raw material in fiber-based material affects the final characteristics because of the deterioration of the original fibers, resulting in reduced mechanical properties, lowered inter-fiber bonding strength, increased fiber defects, loss of molecular mass in the cellulose chain within the fibers, deteriorated swelling ability, and the presence of contaminants (Ren *et al.* 2009). More importantly, the inherent flammability of OCC fiber limits further applications in the preparation of ultra-low density fiberboard (ULDF), which is a promising insulating and packaging material (Cai *et al.* 2016a,b).

There are many ways to improve the flame retardance of fiber substrates, including boron-, nitrogen-, or phosphorus-based fire retardants (Nam *et al*. 2014). However, the use of boron in a high concentration is toxic and creates negative effects in the paper (Nable *et*

al. 1997). The employment of nitrogen-based fire retardants often leads to deteriorations in the mechanical properties of fiber-based materials because of the hygroscopicity of NH_2 groups (Qin *et al.* 2015). Researchers have also tried mixed formulations of aluminum tri-hydrate and sodium borate as a fire retardant in paper, but the low solubility restricted interaction with fibers (Avakian 2014). Water-soluble inorganic salt was instead favored, as water is used in the manufacturing process of ULDF. Aluminum sulfate is one of the most promising candidates because of its excellent fire resistance as well as the cationic nature and high charge density of the aqueous solution (Bo *et al.* 2012). It can be used as the positively charged ingredient in the liquid frothing method, which uses water as medium and mechanical force to introduce air (Xie *et al*. 2008). However, the pre-polymerized aluminum solution remains inferior when there is a high mass ratio of OCC fibers in OCCMs.

Previously, the aggregating power of an aluminum-based solution has been improved by the incorporation of silica. Hasegawa *et al.* (1991) introduced metal ions into polymerized silicic acid solution, which improved the molecular weight, stability, and coagulation performance of the product. More recently, silica incorporation within pre-polymerized metal solutions is used to obtain a larger molecular weight through the application of two techniques. Polymerized silica is introduced to the pre-polymerized metal solution, or a metal solution is introduced to the polymerized silica (Yang *et al.* 2013). Sodium silicate was one of the main raw materials of polymerized silica, and it is relatively cheap and virtually non-toxic. It can be used as a polyelectrolyte and can also be applied economically to wood at industrial wood-preserving operations. Sodium silicate enters voids in the cell lumina and hardens into glass, or it penetrates the interior of porous materials, altering cellular structures and forming many microscopically thin glassy layers. Therefore, using both aluminum sulfate and sodium silicate together in composite polymerizations or separately during OCCM manufacturing may impart fiber-based material with fire retardance and enhanced mechanical properties.

The properties of an Al/Si compound system differs when the aluminum sulfate and sodium silicate are premixed or separately added during OCCM manufacturing. Al/Si compounds have been extensively employed as a retention aid in papermaking (Gyawali and Rajbhandari 2012) and as a flocculant in water treatment (Yang *et al.* 2012; Tolkou *et al.* 2014). The final performance of the product is usually affected by the content of Al/Si compounds, the molar ratio of Al^{3+}/SiO_2, and the different addition form of the Al/Si compounds. However, comprehensive influences on the OCC-based foaming materials have rarely been investigated. Although previous work indicated that the combined addition of Al/Si compounds resulted in better mechanical properties by using virgin kraft pulp (KP) (Chen *et al.* 2014), little information is available on the effect of the content of Al/Si compounds, the molar ratio of Al^{3+}/SiO_2, and different addition forms of Al/Si compounds on fire behavior of OCCMs.

The objectives of this work were to optimize the preparation conditions of the OCCMs using orthogonal testing and to analyze the thermal mechanism of the optimized OCCM. The content of Al/Si compounds, the molar ratio of Al^{3+}/SiO_2, and different addition form of Al/Si compounds were chosen as variables, and LOI and residue percentage of ULDF were selected as indicators. Thermogravimetry (TG), derivative thermogravimetry (DTG), differential scanning calorimetry (DSC), and Fourier transform infrared spectroscopy (FTIR) were conducted to analyze the thermal properties and functional group changes during the thermal decomposition process.

EXPERIMENTAL

Materials

Aluminum sulfate and sodium silicate were purchased from the Tianjin Fuchen Chemical Reagents Factory (Tianjin, China) and used to prepare Al/Si compounds. Polyvinyl alcohol, polyacrylamide, and corn starch were purchased from the Jiangyin Saiwei Technology Trade Co. Ltd (Jiangshu, China) and used to prepare the starch glue. Sodium dodecylbenzene sulfonate (SDBS) and alkyl ketene dimer (AKD) were purchased from the Jiangyin Saiwei Technology Trade Co. Ltd (Jiangshu, China) and used as the surfactant and water repellent, respectively.

Pretreatment of Old Corrugated Containers

The old reclaimed corrugated containers (Yiwu Golden Palace Cardboard Box Factory, Yiwu, China) were soaked in water for 2 h after the elimination of adhesive tapes and nails. OCC was refined in a ZDP32 refiner (Jilin Paper Machinery Manufacturer, Jinlin, China) at 10% consistency until the pulp reached a beating degree of 32°SR. The refined pulp was adjusted to a 6% concentration to be used as a raw material in the manufacture of OCCMs. The fiber morphology of OCC fibers was measured using a MorFi Compact device (1039, Techpap Company, Saint-Martin-d'Hères, France). These results were then compared with those of the virgin kraft pulp (KP) fibers (Table 1).

Table 1. Fiber Morphology of OCC Fibers and Virgin Kraft Pulp (KP) Fiber

Fiber Morphology	OCC Fiber	KP Fiber
Number of Fibers (million/g)	34.54	14.32
Length (um)	1000 (200-4350) *	728 (200-2340) *
Width (um)	26.6 (7-60) *	29.3 (5-60) *
Coarseness (mg/m)	0.0434	0.1189
Cur (%)	11.2	5.7
Broken Ends (%)	41.45	37.09
Fine Elements (% in length)	45.8	45.2
* Values in parentheses mark the data range.		

Compared with virgin KP fiber, OCC fibers were longer and exhibited a lower coarseness and a higher cure rate. These differences in the original properties may have affected the interactions between OCC fibers and Al/Si compounds.

Preparation of Al/Si compounds

The Al/Si compounds with different parameters were prepared according to Table 2. For the combined additions, M1 was obtained by adding the aluminum sulfate solution slowly into the sodium silicate solution and vigorously stirring with a magnetic stir bar; M2 was obtained by adding the sodium silicate solution slowly into the aluminum sulfate solution under vigorous stirring. For separate additions, M3 was denoted as adding sodium silicate first and aluminum sulfate next, while M4 represented adding aluminum sulfate first and sodium silicate second during OCCM manufacturing.

Preparation of OCCMs

The preparation of the OCCMs was conducted as depicted in Fig. 1. All manufacturing parameters were the same except for the details on Al/Si compounds, which

were changed according to the orthogonal test design depicted below. The Al/Si compounds were mixed with absolutely dried OCC pulp (46 g), chlorinated paraffin (30 g), and starch glue (20 mL) in a fiber dissociator (GBJ-A, Changchun Yongxing Test Instrument Factory, Changchun, China). Next, 50 mL of SDBS (10 wt%) was introduced into the mixture and allowed to froth for another 5 min. The foams were controlled to within three fourths of the foaming tank, and AKD (50 mL) was added into the froth system, foaming for another 2 min to the desired height. The obtained foam was poured into a cubic mold of 200 mm × 200 mm × 50 mm ($L \times W \times H$) for dehydration. The mold was dried in an oven at 103 °C until the mixture reached a constant moisture content.

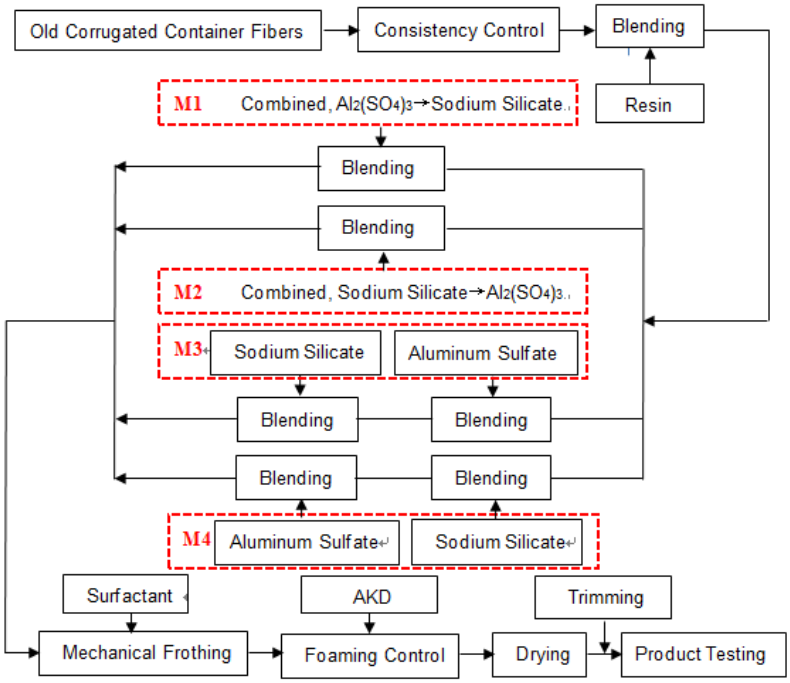

Fig. 1. Preparation of old corrugated container fiber foam material (OCCM)

Orthogonal Test Design

Various factors representing important effects on the LOI and residue percentage of OCCMs were determined based on the exploratory trials. The mole ratio of Al^{3+}/SiO_2, the amount of Al/Si compounds, and the addition form were chosen as variables, and LOI and residue percentage of ULDF were selected as indicators when designing an L16 orthogonal experiment (4^5) with three factors and four levels, as shown in Table 2.

Table 2. Factors and Levels of Orthogonal Test

Level	Factor		
	Al/Si Compound Content (*A*, mL)	Al^{3+}/SiO_2 Molar Ratio(*B*)	Addition Form of Al/Si Compounds(C)
1	700	1:0.50	M1
2	800	1:0.75	M2
3	900	1:1.00	M3
4	1000	1:1.25	M4

Characterization

Particle size of Al/Si compounds

The distribution of the particle sizes in the dispersion was determined using a laser particle size analyzer (BT-9300H, Bettersize Instruments Ltd., Dandong, China) at a refraction coefficient of 1.33 and a scattering angle of 90°. A droplet of the Al/Si compounds (M1 and M2) was diluted in 20 mL of water to measure the particle size distribution.

Limiting oxygen index (LOI)

The LOI was measured using an HC-2 oxygen index meter (Jangning Factory, Nanjing, China) at room temperature. The specimens were cut into dimensions of 120 mm × 10 mm × 10 mm, according to GB/T 2406.2 (2009). All reported results are the average of ten replicates.

Residue percentage

The residue of each sample was obtained in a muffle furnace at a nitrogen airflow of 2 L/min for 20 min at 400 °C. The residue percentage was calculated as Eq.1,

$$\text{Residue percentage (\%)} = (m_0 - m_1)/m_0 \times 100 \quad (1)$$

where m_0 represented the initial mass (g) and m_1 represented the residue mass (g) of OCCM. All of the results were the average of three replicates.

Thermal analysis

Thermal analyses of OCCMs (8 ± 1 mg) were conducted using a Netzsch STA449F3 thermo-analyzer instrument (Selb, Germany). The thermograms were obtained between 25 °C and 600 °C at a heating rate of 10 °C /min in a nitrogen atmosphere, with a flow rate of 10 mL/min. The temperature and mass were accurate to ± 1 °C and ± 0.2%, respectively.

Fourier transform infrared (FTIR) spectroscopy analysis

The FTIR spectra were recorded on a Nicolet 380 spectrometer (Thermo Fisher Scientific, Waltham, MA, USA). The control and optimized OCCMs were characterized using a tablet compressing technique with a 1:100 ratio of sample to KBr by mass. All samples, except for the original, were placed in a muffle furnace until they reached temperatures of 200, 300, 400, 500, or 600 °C.

RESULTS AND DISCUSSION

Orthogonal Test Results Analysis

OCCMs were produced according to the orthogonal test design, and the corresponding LOI and residue percentage were recorded (Table 3). The range analysis of LOI and residue percentage is shown in Table 4. According to the *K* value in Table 4, the optimal level for each factor on both LOI and residue percentage was A_3, B_3, and C_3. The importance of the factors on LOI and residue percentage was $C > B > A$. Thus, the optimum conditions for this procedure can be expressed as $A_3B_3C_3$, where *A*, *B*, and *C* represent the

Al/Si compound content, the molar ratio of Al^{3+}/SiO_2, and the addition form of Al/Si compounds, respectively.

Table 3. Scheme and Results of Orthogonal Experiment

Run No.	Factors						
	A(mL)	*B*	*C*	Control 1	Control 2	LOI	Residue percentage (%)
1	1	1	1	1	1	30.5	46.05
2	1	2	2	2	2	27.5	48.77
3	1	3	3	3	3	31.7	51.99
4	1	4	4	4	4	30.0	48.36
5	2	1	2	3	4	28.0	49.64
6	2	2	1	4	3	27.5	46.74
7	2	3	4	1	2	28.8	50.76
8	2	4	3	2	1	31.0	53.29
9	3	1	3	4	2	30.0	48.00
10	3	2	4	3	1	29.0	50.02
11	3	3	1	2	4	31.5	52.85
12	3	4	2	1	3	30.0	54.23
13	4	1	4	2	3	29.0	51.19
14	4	2	3	1	4	31.0	54.43
15	4	3	2	4	1	29.5	50.26
16	4	4	1	3	2	32.5	49.04

Table 4. Range Analysis of LOI and Char Yield

Factor	Indicator	$\overline{K}_1$	$\overline{K}_2$	$\overline{K}_3$	$\overline{K}_4$	R_i	Importance of Factors
A	LOI	29.8	28.6	30.1	29.5	1.69	*C* > *B* > *A*
B		29.3	28.7	30.8	30.3	2.13	
C		30.50	28.7	30.8	29.2	2.19	
d		30.0	29.7	30.3	29.2	0.76	
e		30.0	29.7	29.5	30.1	0.56	
A	Residue percentage	48.79	50.11	51.27	51.23	2.48	*C* > *B* > *A*
B		48.72	49.94	51.46	51.24	2.75	
C		48.67	50.72	51.93	50.08	3.26	
Control 1		51.37	51.52	50.17	48.34	0.89	
Control 2		49.91	49.14	51.04	51.32	0.18	

$\overline{K}_1$ is defined as the average of the evaluation indices of level 1, the same as $\overline{K}_2$, $\overline{K}_3$, and $\overline{K}_4$. R_i is the range of all levels, which is used for evaluating the importance of the factors. *i.e.* a larger R_i means a greater importance of the factor.

Table 5 shows the variance analysis of LOI and residue percentage of OCCMs. At 95% confidence, the effect of factor A on both LOI and residue percentage was significant, whereas under 99% confidence levels, the effect of factor B and C on both LOI and residue percentage was significant. This result is in accordance with the range analysis discussed above.

Table 5. Variance Analysis of LOI and Residue Percentage

Indicator	Sources of variance	S_j	f	f_j	F0.95 (3, 6)	F0.99 (3, 6)
LOI	A	6.33	3	7.64	4.76*	9.78
	B	11.05	3	13.34	4.76	9.78*
	C	13.02	3	15.72	4.76	9.78*
	Error	0.83	6	-	-	-
Residue Percentage	A	16.46	3	8.61	4.76*	9.78
	B	19.22	3	10.05	4.76	9.78*
	C	22.09	3	11.56	4.76	9.78*
	Error	1.83	6	-	-	-
S_j, f_j, and * represent the squared error, degrees of freedom, and the significance of the factors, respectively.						

Effect of Various Factors on the LOI and Residue percentage of OCCMs

The trend charts of the effect analysis of test factors on LOI and residue percentage for OCCMs are shown in Fig. 2. Figure 2a shows that the LOI and residue percentage of OCCMs increased initially and then decreased slightly with the increasing content of Al/Si compounds. This result may be due to insufficient Al/Si compounds, such that they were incapable of acting as bridges or connectors between fibers and colloidal particles, resulting in a thinner film or an incomplete wrapping of fibers (Cai *et al.* 2014).

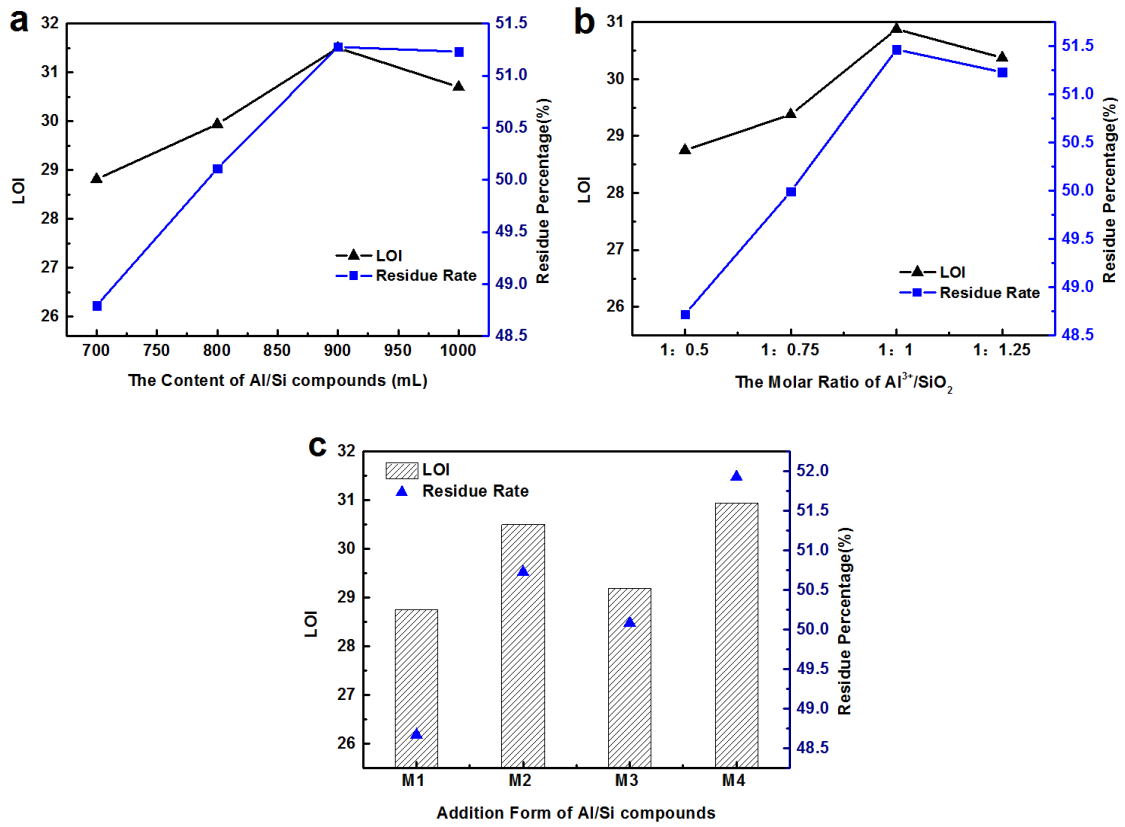

Fig. 2. Effect of (a) the content of Al/Si compounds, (b) molar ratio of Al^{3+}/SiO_2, and (c) addition form of Al/Si compounds on the limiting oxygen index (LOI) and residue percentage of OCCM

However, when the content of Al/Si compounds in the foaming system was more than 900 mL, a smaller LOI and residue percentage was obtained. Increasing the content of Al/Si compounds to within 900 mL improved the LOI and residue percentage of OCCMs. A moderate content of Al/Si compounds may produce a compact adsorption layer, resulting in the highest LOI and residue percentage.

Figure 2b implies that the LOI and residue percentage increased first and then decreased as the molar ratio Al^{3+}/SiO_2 increased. When the molar ratio of Al^{3+}/SiO_2 was lower, the electronegative polysilicic acid played a more active role in the foaming system than the positively charged aluminum sulfate. The reduced neutralizing capacity between polysilicic acid and the fibers gave rise to the poor flocculation of Al/Si compounds on the fiber surface and the poor fire retardance of the OCCMs (Xu *et al.* 2012). In contrast, a higher Al^{3+}/SiO_2 molar ratio resulted in a more positively charged aluminum sulfate, and higher adsorption and bridging with fibers. This may have induced the repulsive interaction between positively charged fibers and cationic Al/Si compounds, and the poor flocculation of Al/Si compounds on the fiber surface (Paren and Vapaaoksa 1995). Therefore, an optimized LOI and residue percentage was obtained when the Al/Si compounds exerted not only the adsorption and bridging effect, but also the neutralization effect in the foaming system.

Figure 2c depicts the effect of addition form of the Al/Si compounded system on the LOI and residue percentage of OCCMs. The fine fibers could have initially been neutralized by aluminum sulfate during the OCCM making (M4), and even been endowed with a positive charge, which may have promoted the hydrolysis of sodium silicate introduced later (Jabbari *et al.* 2016). Simultaneously, part of the Al^{3+} may penetrate or enter the micropores of fibers, facilitating the fire retardance of OCCM. In this condition, the following $H_3SiO_4^+$ and $H_4SiO_4^{2+}$ hydrolysis by sodium silicate can be well connected with the bonding point of aluminum sulfate on the fiber surface and deposit on the fiber surface. Additionally, the molecular chains of polysilicic acid may stretch outward from the bonding point and bridge with the fibers. In contrast, adding the sodium silicate first (M3) induced a mutual repulsion between sodium silicate hydrolysates and fibers, as the waste fibers usually contains a lot of anionic trash, which cannot connect well to the hydrolysates of sodium silicate, resulting in a lower LOI and residue percentage. The particle size of the combined addition was much higher than that of the micropores when the microfibrils were under the swelling condition for M1 and M2 (Table 6). Thus, the connection may only rely on the charge neutralization, adsorption, and bridging effect on fibers. Therefore, M4 exhibited the most noticeable impact on the LOI and residue percentage of OCCMs.

Table 6. Particle Size of Hydrated Ion and Al/Si Compounds

Type	$[Al(H_2O)]^{3+}$	$[Na(H_2O)n]^+$ n = 1, 2, 3 or 4	M 1	M 2
Mean particle size (nm)	0.48	0.36	46 490	40 630

In sum, based on the LOI and residue percentage, the best combination of various factors was $A_3B_3C_3$. Namely, the content of Al/Si compounds was 900 mL, the molar ratio of Al^{3+}/SiO_2 was 1:1, and the M4 addition form was used. Under these conditions, further experiments were conducted with average values for LOI at 32.3 ± 0.2 (which met the GB 8624 (2012)), and an average residue percentage at 53.51 ± 0.36 %, which was close to the

optimized results in the orthogonal experiment. These results confirmed that the optimized combination was feasible.

Thermal Analysis

To investigate the changes in weight and heat release of OCCMs, TG, DTG, and DSC curves of the control and optimized OCCMs are presented in Fig. 3.

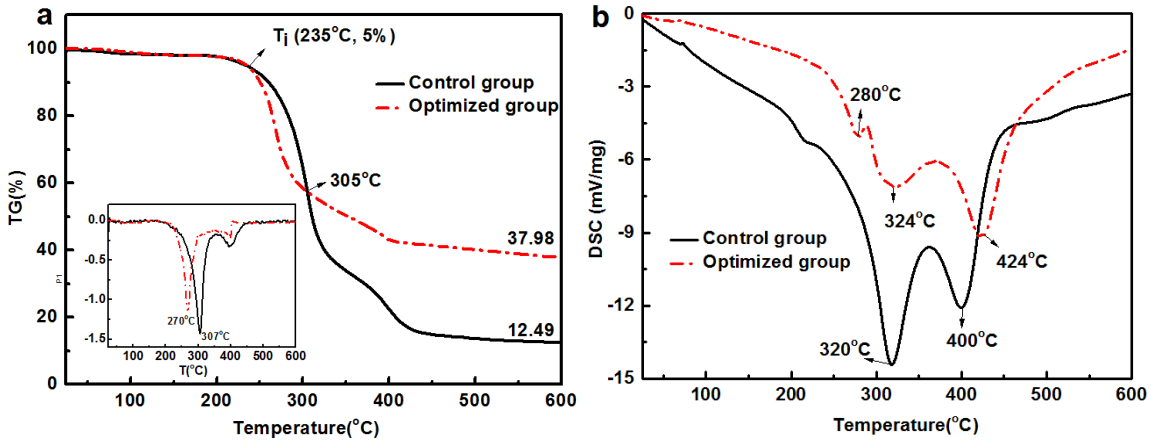

Fig. 3. (a) Thermogravimetry (inset: derivative thermogravimetric curves); and (b) differential scanning calorimetry curves of the control and optimized OCCMs

There were three distinct stages in the TG curves of the control and optimized groups (Fig. 3a). Stage I (room temperature to about 235 °C) represented dehydration, in which free water in the specimens evaporated. Mass loss during this period was around 5%. Stage II (235 to 397 °C) was where the most mass loss occurred (77% for the control group and 57% for the optimized group). Mass loss was mainly caused by the thermal degradation of hemicellulose and cellulose into char residues, CH_4, CH_3OH, and CH_3COOH (Chapple and Anandjiwala 2010). In this range, the mass loss rate of the optimized group was faster than the control OCCMs before 305 °C. This result may reflect the possibility that acid species such as $Al_2(SO_4)_3$ may catalyze cellulose dehydration as char-promoters in the condensed phase. Some slight mass loss occurred during Stage III (397 to 650 °C), primarily due to the degradation of lignin. Additionally, Fig. 3a indicates that the initial decomposition temperature (T_i, 5% mass loss) of the control OCCMs was the same as that of the optimized one at 235 °C. However, The maximum degradation temperatures (T_m) of the optimized OCCMs (270 °C) was lower than the control (307 °C), indicating that Al/Si compounds encouraged the degradation of OCCM at lower temperatures *via* dehydration and the formation of carbonaceous char and water. This result was confirmed by the enhanced residue percentage of the optimized group (37.98%) compared with that of the control group (12.49%).

The DSC curve of the control OCCMs (Fig. 3b) presents a heat release decomposition bimodal profile, which clearly degraded at about 320 and 400 °C. However, the heat release of the optimized OCCMs indicated three peaks at 280, 324, and 400 °C. The heat release of the optimized group was much lower than that of the control in most of the thermal decomposition process, indicating the heat absorption of Al/Si compounds of the optimized group during decomposition. Therefore, the addition of Al/Si compounds

facilitates residue weight and reduces the heat release of the optimized OCCMs during depolymerisation.

FTIR Analysis

To further explore changes in functional groups during thermal pyrolysis, FTIR spectra were collected at different temperatures (Fig. 4). In the FTIR spectrum of the control OCCMs, all the characteristic absorption bands of cellulose were observed at room temperature (Fig. 4a). The -OH was observed at a broad absorption band ranging from 3700 to 3100 cm^{-1}; C-H stretching was observed from 2800 to 3000 cm^{-1} (Schmitt and Flemming 1998). The FTIR spectrum of the optimized OCCMs (Fig. 4b) was similar to that of the control. The additional peaks at 1050, 792, and 649 cm^{-1} were ascribed to the antisymmetric stretching vibration of Si-O-Si, Al-O-Si, and Al-OH, respectively. The peak at 467 cm^{-1} was the bending vibration of Si-O-Si (Schmitt and Flemming 1998). These peaks proved that Al/Si compounds were present on the fiber surface of the optimized OCCM.

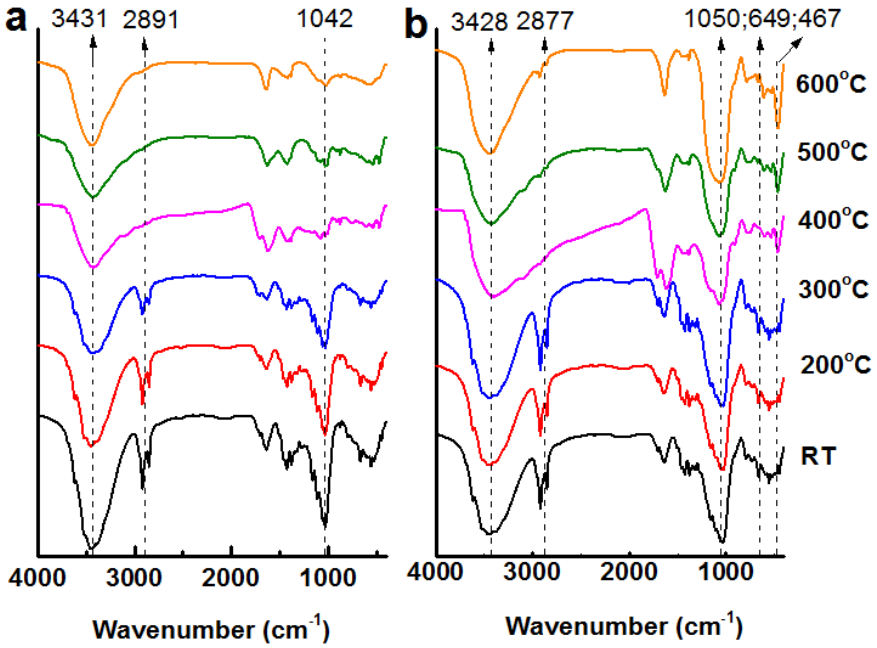

Fig. 4. Fourier transform infrared spectroscopy of (a) the control group and (b) the optimized group at different temperatures. RT abbreviation stands for room temperature.

However, the 1042 cm^{-1} absorbance ascribed to C-O group noticeably weakened at 300 °C (Fig. 4a), suggesting the decomposition of hemicellulose. The cellulose C-H stretching vibration at 2891 cm^{-1} disappeared at 400 °C, indicating cellulose decomposition. These results were in accordance with the TGA analysis. In the control group, the relative absorbance of the cellulose hydroxyl band at 3431 cm^{-1} decreased with increasing temperature, while in the optimized OCCMs, this peak did not change noticeably. All characteristic absorbance patterns of Al/Si compounds were observed in the optimized OCCMs. Taken together, the TG, DTG, and DSC analyses showed that pyrolysis of the optimized OCCMs was affected by Al/Si compounds.

CONCLUSIONS

1. This study showed that an aluminum sulfate/sodium silicate compounded system can be used as a fire retardant in OCCM manufacturing under appropriate process conditions.
2. The optimum conditions determined by orthogonal experiments were a 900 mL content of Al^{3+}/SiO_2, a 1:1 molar ratio of Al^{3+}/SiO_2, and separately adding aluminum sulfate solution first and sodium silicate solution next. The LOI and residue percentage of the optimized OCCM were 32.3 and 53.51%, respectively, which meets the national standards of construction material (GB 8624 (2012)).
3. FTIR analysis showed that there were new functional groups in the optimized OCCMs. These groups encouraged the dehydration of OCC fibers at lower temperatures and promoted char formation in OCCMs, as shown in the thermogravimetry analysis. Compared with the control group, the residue percentage of optimized OCCM increased from 12.49% to 37.98%.

ACKNOWLEDGMENTS

The authors thank the Natural Science Foundation of China (NSFC) (No. 30871982) and the National Key Program of China (2008BADA9B01) for financial support.

REFERENCES CITED

Avakian, R. W. (2014). "Blends of nanocomposites and their use," U.S. Patent No. 8,674,010.

Bo, X., Gao, B., Peng, N., Wang, Y., Yue, Q., and Zhao, Y. (2012). "Effect of dosing sequence and solution pH on floc properties of the compound bioflocculant-aluminum sulfate dual-coagulant in kaolin-humic acid solution treatment," *Bioresource Technology* 113, 89-96. DOI: 10.1016/j.biortech.2011.11.029

Cai, L. L., Xie, Y. Q., Zhuang, Q. P., and Niu, M. (2014). "Effects of polysilicate aluminum sulfate on fire resistance of ultra-low density materials," *Journal of Beijing Forestry University* 36(5), 136-141. DOI: 10.13332/j.cnki.jbfu.2014.05.002

Cai, L. L., Fu, Q. L., Niu, M., Wu, Z. Z, and Xie, Y. Q. (2016a). "Effect of chlorinated paraffin nanoemulsion on the microstructure and water repellency of ultra-low density fiberboard," *BioResources* 11(2), 4579-4592. DOI: 10.15376/biores. 11. 2. 4579-4592

Cai, L. L., Zhuang, B. R., Huang, D. B, Wang, W., Niu, M., Xie, Y. Q., and Wang, X. D. (2016b). "Ultra-low density fibreboard with improved fire retardance and thermal stability using a novel fire-resistant adhesive," *BioResources* 11(2), 5215-5229. DOI: 10.15376/biores. 11. 2. 5215-5229

Chapple, S., and Anandjiwala, R. (2010). "Flammability of natural fiber-reinforced composites and strategies for fire retardancy: A review," *Journal of Thermoplastic Composite Materials* 23(6), 871-893. DOI: 10.1177/0892705709356338

Chen, T., Niu, M., Xie, Y., Wu, Z., Liu, X., Cai, L., and Zhuang, B. (2014). "Modification of ultra-low density fiberboards by an inorganic film formed by Al/Si deposition and their mechanical properties," *BioResources* 10(1), 538-547. DOI: 10.15376/biores.10.1.538-547

Chen, Y., Wan, J., Ma, Y., Tang, B., Han, W., and Ragauskas, A. J. (2012). "Modification of old corrugated container pulp with laccase and laccase–mediator system," *Bioresource Technology* 110, 297-301. DOI: 10.1016/j.biortech.2011.12.120

GB/T2406.2 (2009). "Standard test method for measuring the minimum oxygen concentration to support candle-like combustion of plastics," Standardization Administration of China, Beijing, China.

GB 8624 (2012). "Classification for burning behavior of building materials and products," Standardization Administration of China, Beijing, China.

Gyawali, G., and Rajbhandari, A. (2012). "Investigation on coagulation efficiency of polyaluminium silicate chloride (PASiC) coagulant," *Scientific World* 10(10), 33-37. DOI: 10.3126/sw.v10i10.6859

Hasegawa, T., Hashimoto, K., Onitsuka, T., Goto, K., and Tambo, N. (1991). "Characteristics of metal-polysilicate coagulants," *Water Science and Technology* 23(7-9), 1713-1722.

Heydari, S., Ghasemian, A., and Afra, E. (2013). "Effects of refining and cationic polyacrylamide on strength properties of paper made from old corrugated container (OCC)," *World of Sciences Journal*, Special Issue.

Iler, R. K. (1952). "Association between polysilicic acid and polar organic compounds," *The Journal of Physical Chemistry* 56(6), 673-677. DOI: 10.1021/j150498a001

Jabbari-Hichri, A., Bennici, S., and Auroux, A. (2016). "Effect of aluminum sulfate addition on the thermal storage performance of mesoporous SBA-15 and MCM-41 materials," *Solar Energy Materials and Solar Cells* 149, 232-241. DOI: 10.1016/j.solmat.2016.01.033

Nable, R. O., Bañuelos, G. S., and Paull, J. G. (1997). "Boron toxicity," *Plant and Soil* 193(12), 181-198. DOI: 10.1007/978-94-011-5580-9_12

Nam, S., Condon, B. D., Foston, M. B., and Chang, S. (2014). "Enhanced thermal and combustion resistance of cotton linked to natural inorganic salt components," *Cellulose* 21(1), 791-802. DOI: 10.1007/s10570-013-0133-y

Paren, A., and Vapaaoksa, P. (1995). "Polysilicic acid containing aluminum silicate in cellulose support; fireproof fibers and textiles," U.S. Patent 5,417,752.

Qin, Z., Li, D., Lan, Y., Li, Q., and Yang, R. (2015). "Ammonium polyphosphate and silicon-containing cyclotriphosphazene: Synergistic effect in flame-retarded polypropylene," *Industrial and Engineering Chemistry Researc*h 54(43), 10707-10713. DOI: 10.1021/acs.iecr.5b02343

Rahmaninia, M., and Khosravani, A. (2015). "Improving the paper recycling process of old corrugated container wastes," *Cellulose Chemistry and Technology* 49, 203-208.

Ren, J., Peng, F., and Sun, R. (2009). "The effect of hemicellulosic derivatives on the strength properties of old corrugated container pulp fibers," *Journal of Biobased Materials and Bioenergy*, 3(1), 62-68. DOI: 10.1166/jbmb.2009.1008

Schmitt, J., and Flemming, H. C. (1998). "FTIR-spectroscopy in microbial and material analysis," *International Biodeterioration and Biodegradation* 41(1), 1-11. DOI: 10.1016/S0964-8305(98)80002-4

Tang, Y., Shen, X., Zhang, J., Guo, D., Kong, F., and Zhang, N. (2015). "Extraction of cellulose nano-crystals from old corrugated container fiber using phosphoric acid and

enzymatic hydrolysis followed by sonication," *Carbohydrate Polymers* 125, 360-366. DOI: 10.1016/j.carbpol.2015.02.063

Tolkou, A., Zouboulis, A., and Peleka, E. (2014). "Novel pre-polymerized coagulant agents used for the treatment of industrial wastewaters," in: *1st IWA Specialized International Conference: EcoSTP-Eco Technologies for Wastewater Treatment*, Santiago de Compostela, Spain, p. 6.

Xie, Y. Q., Tong, Q. J., and Chen, Y. (2008). "Construction mechanism of reticular structure of plant fiber," *Journal of Korea Furniture Society* 19(2), 106-110.

Xu, W., Gao, B., and Wang, Y. (2012). "Influences of polysilicic acid in Al_{13} species on floc properties and membrane fouling in coagulation/ultrafiltration hybrid process," *Chemical Engineering Journal* 181, 407-415. DOI: 10.1016/j.cej.2011.11.107

Yang, Z., Gao, B., Wang, Y., Zhao, Y., and Yue, Q. (2012). "Fractionation of residual Al in natural water treatment from reservoir with poly-aluminum-silicate-chloride (PASiC): Effect of OH/Al, Al/Si molar ratios and initial pH," *Journal of Environmental Sciences* 24(11), 1908-1916. DOI: 10.1016/s1001-0742(11)61059-0

Yang, Z., Liu, B., Gao, B., Wang, Y., and Yue, Q. (2013). "Effect of Al species in polyaluminum silicate chloride (PASiC) on its coagulation performance in humic acid-kaolin synthetic water," *Separation and Purification Technology* 111, 119-124. DOI: 10.1016/j.seppur.2013.03.040

Article submitted: March 18, 2016; Peer review completed: May 28, 2016; Revised version received and accepted: June 1, 2016; Published: June 20, 2016.
DOI: 10.15376/biores.11.3.6505-6517